

Magnetically induced explosion of a giant vortex state in a mesoscopic superconducting disk

D. S. Golubović*, M. V. Milošević§, F. M. Peeters§ and V. V. Moshchalkov*

**Nanoscale Superconductivity and Magnetism Group,
Laboratory for Solid State Physics and Magnetism,*

K. U. Leuven, Celestijnenlaan 200 D, B-3001 Leuven, Belgium

*§Departement Fysica, Universiteit Antwerpen (Campus Drie Eiken),
Universiteitsplein 1, B-2610 Antwerpen, Belgium*

The nucleation of superconductivity in a superconducting disk with a Co/Pt magnetic triangle was studied. We demonstrate that when the applied magnetic field is parallel to the magnetization of the triangle, the giant vortex state of vorticity three splits into three individual Φ_0 -vortices, due to a pronounced influence of the C_3 symmetry of the magnetic triangle. As a result of a strong pinning of the three vortices by the triangle, their configuration remains stable in a broad range of applied magnetic fields. For sufficiently high fields, Φ_0 -vortices merge and the nucleation occurs through the giant vortex state. The theoretical analysis of this novel reentrant behaviour at the phase boundary, obtained within the Ginzburg - Landau formalism, is in excellent agreement with the experimental data.

PACS numbers: 74.78.Na., 75.75.+a, 74.25.Dw

The nucleation of superconductivity in mesoscopic samples, whose dimensions are comparable to the superconducting coherence length $\xi(T)$ and the penetration depth $\lambda(T)$, is substantially affected by the sample boundary (see Ref. [1] and references therein). It is well established that in circular mesoscopic disks and loops the onset of superconductivity mostly occurs through the giant vortex state (GVS) due to their cylindrical symmetry [2]. On the other hand, in superconducting squares and triangles for certain magnetic fields the GVS easily splits into individual Φ_0 -vortices (Φ_0 is the superconducting flux quantum), with a possible generation of additional antivortices [3]. The transition from the GVS to a set of Φ_0 -vortices is caused by the reduced axial symmetry of squares and triangles and ensures that a vortex pattern conforms to the symmetry imposed by the boundary of the sample.

In this paper we investigate the onset of superconductivity in a mesoscopic disk on which a magnetic triangle with out-of-plane magnetization is placed. The nucleation of superconductivity in hybrid superconductor/ferromagnet disks and loops has been studied previously, both experimentally and theoretically, as these are a good model system to gain insight into the interplay between superconductivity and magnetism in the context of magnetic vortex pinning and related phenomena [5, 6, 7, 8]. In this paper we show that the *symmetry* of the magnetic triangle has a profound effect on the onset of superconductivity in the disk. Due to the competition between the cylindrical symmetry of the superconducting disk and the C_3 symmetry of the stray field, superconductivity nucleates as a GVS for vorticity $L = 2$, whereas for $L = 3$ the GVS splits into three Φ_0 -vortices. As a result of a strong pinning of the three individual vortices their configuration remains stable in a broad range of applied magnetic fields. For sufficiently high fields, Φ_0 -vortices merge and the nucleation occurs through the giant vortex state. The theoretical analysis of this novel reentrant behaviour at the phase boundary, obtained within the Ginzburg - Landau formalism, is in excellent agreement with the experimental data.

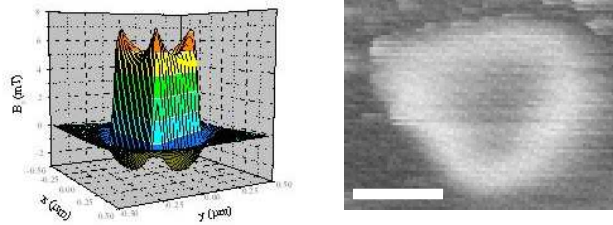


FIG. 1: The calculated spatial profile (a) of the stray field and (b) a magnetic force micrograph of the triangle. The field values were calculated using the saturation magnetization of bulk Co.

The sample was prepared by electron beam lithography, using double resist technique and lift-off in two steps. For details we refer to Ref. [6]. In the first step 30 nm Al disks were prepared using thermal evaporation. Upon the alignment, in the second step Co/Pt magnetic triangles with the designed size of 650 nm were grown by electron beam evaporation on the disks. Some disks were left without magnetic elements to be used as reference samples. The Co/Pt magnetic triangle consists of a 2.5 nm Pt buffer layer a 10 bi-layers of Co and Pt with the thicknesses of 0.4 nm and 1 nm, respectively. The triangle is separated from the superconducting disk by a 2 nm Si spacer layer to avoid the proximity effect and suppression of the order parameter in the disk below the magnetic triangle. Co/Pt multi-layers are known to have a pronounced perpendicular (out-of-plane) anisotropy, caused by the surface anisotropy between

Co and Pt layers, and a high remanence [9]. The coercive field of the co-evaporated reference film is 170 mT at room temperature, with a 90 % remanence. The calculated spatial profile of the stray field $B_z(x, y)$ generated by the triangle is shown in Fig. 1. Prior to the measurements the triangle was saturated along the easy axis in a high magnetic field. Therefore, it has been assumed that applied magnetic fields in the range ± 15 mT did not affect the magnetization of the triangle during the measurements.

A scanning electron micrograph of the structure is shown in Fig. 2. The radius of the disk is $1.34 \mu\text{m}$, which exceeds approximately 3 % the patterned radius. Even though the triangle was designed as equilateral, its sides are 690 nm, 650 nm and 740 nm, due to a relatively low acceleration voltage and a lack of the proximity correction tool in our e-beam system.

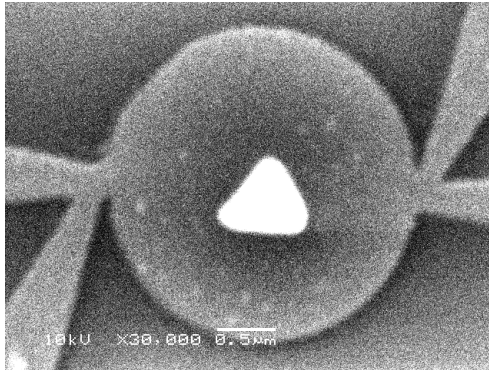


FIG. 2: A scanning electron micrograph of the structure.

The superconducting $T_c(B)$ phase boundary was obtained by four-point transport measurements in a ^4He cryogenic setup at temperatures down to 1.25 K with the temperature stability of 0.4 mK, applying the magnetic field perpendicularly to the sample surface. A transport current with the effective value of 100 nA and frequency 27.7 Hz was used. The measurements were taken by sweeping the magnetic field at a constant temperature. The temperature and field steps were 0.5 mK and $50 \mu\text{T}$, respectively. A special attention was being paid to eliminate any possible trapped flux in the set-up during the measurements. The room temperature resistance and the residual resistance at 4.2 K of the structure shown in Fig. 2 are 6.5Ω and 3.2Ω , respectively. The mean free path of Al, estimated from the co-evaporated reference film, is 12.3 nm, so that the samples are in the dirty limit with the coherence length $\xi(0) = 120$ nm. The critical temperature of the disk with the triangle in zero applied field is $T_{c0} = 1.4136$ K, whereas for the reference disk is $T_{c0}^{(R)} = 1.4366$ K.

Hereafter we will be referring to a magnetic field applied parallel to the magnetization of the triangle as positive.

The experimental superconducting $T_c(B)$ phase boundary is shown in Fig. 3. The inset is a part of the $T_c(B)$ phase boundary of a reference superconducting disk, without the magnetic triangle, down to $0.967 T_{c0}^{(R)}$. The shift of the $T_c(B)$ phase boundary along the field axis, with the maximum critical temperature T_{cm} attained for a finite value of an applied magnetic field, was already previously observed and is caused by the compensation of the stray field generated by the dot [6, 7]. It can be seen that for negative applied fields the $T_c(B)$ phase boundary exhibits a typical cusp-like behaviour in the whole temperature range, with each cusp corresponding to a change in vorticity by one. However, for positive applied fields there are no cusps in the $T_c(B)$ phase boundary for a broad range of temperatures between $0.991 T_{cm}$ and $0.969 T_{cm}$. The region is indicated by a dashed square in Fig. 3. For lower temperatures, the cusp-like behaviour is recovered. In the same relative temperature range, the $T_c(B)$ phase boundary of a reference superconducting disk exhibits the typical behaviour [4].

The experimental data were analyzed in the framework of the Ginzburg-Landau (GL) theory. The 3D GL equations were solved numerically, without imposing any constraints on the final form of the order parameter at a given temperature and magnetic field (for details of the approach, see Ref. [10] and references therein). At the superconductor/vacuum interface the Neumann boundary condition for the order parameter was used. The influence of the current and voltage contacts on the nucleation process was modelled by adding two stripes with length of 400 nm and width of 250 nm to the disk, at the position of the current contacts. Even though they geometrically differ from the real contacts, they allow for a slight local spread of the screening currents in the disk, as well as provide a local enhancement of the superconductivity in the contact area. Therefore, they may be used to adequately describe the physical phenomena related to the real contacts. The simulations were carried out with the exact dimensions of the disk and triangle, using the saturation magnetization of bulk Co $m = 140$ mT, with the coherence length as a fitting parameter. The experimental results were theoretically best reproduced with $\xi(0) = 118$ nm, which is in excellent agreement with the coherence length obtained for the reference film.

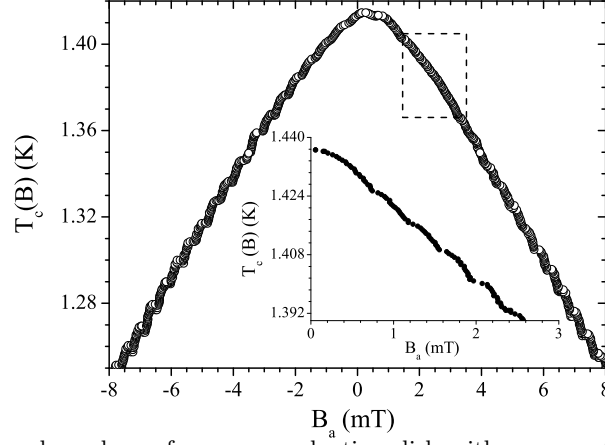


FIG. 3: Experimental $T_c(B)$ phase boundary of a superconducting disk with a magnetic triangle on top. Dashed square indicates the temperature region where no cusps in the phase boundary are observed. The inset shows a part of the $T_c(B)$ phase boundary of a reference disk down to 1.39 K.

Fig. 4 shows the experimental and theoretical $T_c(B)$ phase boundaries of the disk with the triangle, down to $0.95 T_{cm}$. Open symbols are the experimental data, whereas the solid line presents the theoretically obtained phase boundary. The numbers indicate vorticities and arrows point the field values at which a particular transition occurs. The inset shows the $dT_c(B)/dB_a$ versus the applied field B_a . The stray field of the triangle creates one vortex in

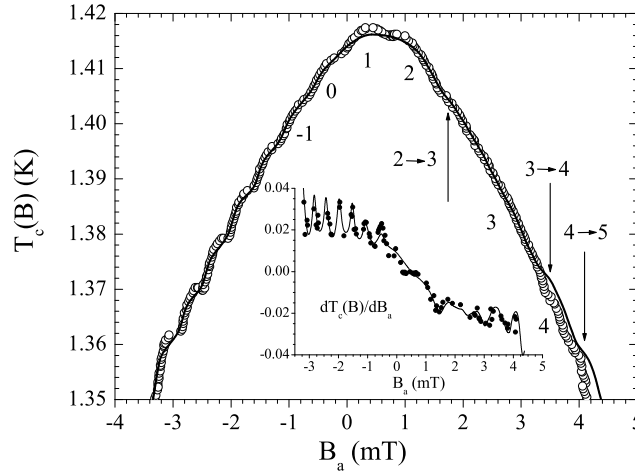


FIG. 4: $T_c(B)$ phase boundary of a superconducting disk with a magnetic triangle. The solid line presents the theoretical curve, whereas open symbols show experimental data. Numbers stand for the vorticity, with arrows indicating the transitions between the states with different vorticities. The inset shows the $dT_c(B)/dB_a$ versus the applied field. Filled symbols are experimental data and line is the theoretical curve.

the disk in the absence of the external magnetic field. The state without vortices ($L = 0$) is, therefore, realized by applying small negative magnetic fields. For negative applied fields, the nucleation of superconductivity occurs through the GVS, which is reflected by a regular cusp-like character of the $T_c(B)$ phase boundary. The contour plot of the phase of the order parameter for $L = -3$, shown in Fig. 5, illustrates the presence of the GVS.

The GVS is retained in positive applied fields for up to $L = 2$. However, for vorticity $L = 3$ the lowest energy state corresponds to three Φ_0 -vortices. The contour plots of the phase of the order parameter for the $L = 2$ and $L = 3$ are shown in Fig. 5. It is clear that the state $L = 2$ is a GVS located below the triangle, whereas for $L = 3$ there are three individual vortices, located towards the apices of the triangle. The three Φ_0 vortices are strongly pinned at their positions by the magnetic triangle. This results in a substantially enhanced stability of the $L = 3$ state, and gives rise to an extended cusp in the $T_c(B)$ phase boundary. The configuration of the three cornered vortices is imposed by the symmetry and remains stable for $L = 4$ and $L = 5$. For higher applied fields (and consequently higher vorticities), vortices are compressed under the triangle at the centre of the disk and forced by the screening currents to merge back to the GVS. This reentrant-like behaviour is reflected by the reappearance of regular cusps in the $T_c(B)$ phase boundary for higher fields (see Fig. 3).

Obviously, in addition to the character and symmetry of the boundary, the onset of superconductivity in hybrid

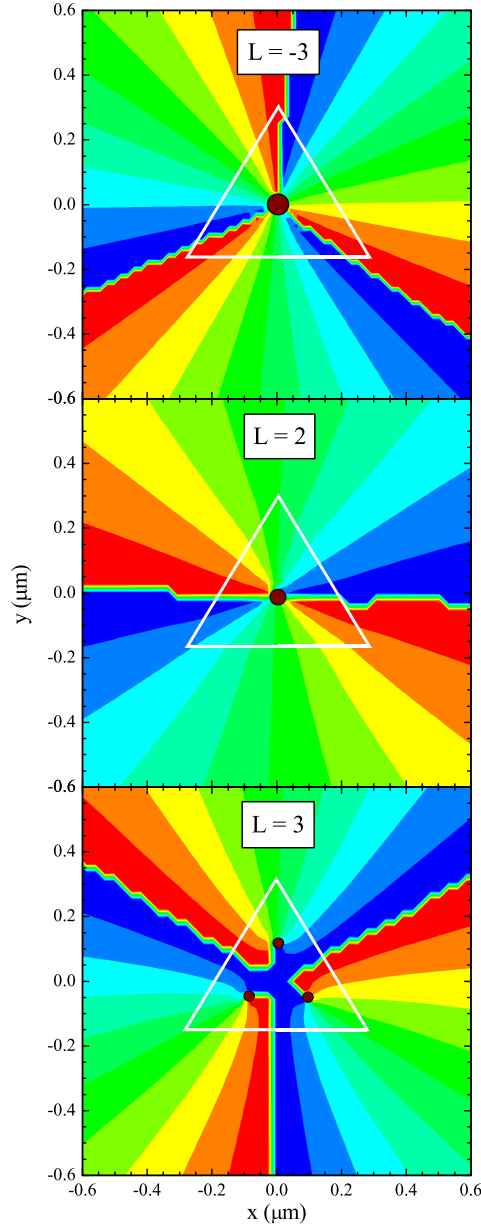


FIG. 5: The contour plot of the phase of the order parameter for the vorticities $L = -3$, $L = 2$ and $L = 3$. Blue/red colour are $0/2\pi$ of the phase. The white triangle illustrates the position of the magnetic triangle.

superconductor/ferromagnet structures is profoundly influenced by the stray field locally generated by the magnetic element. The extent of the influence depends on the mutual relation between the parameters of the superconductor and the ferromagnet. As detailed in Ref. [11], in the theory of vortex pinning by perpendicularly magnetized dots, the lowest energy state is achieved when an external vortex is located below the dot (in the parallel case), whereas an eventual anti-vortex would be repelled and its equilibrium position is determined by other relevant parameters. As a general rule, the prevailing mechanism which governs the vortex behaviour is its interaction with the screening currents generated by the stray field of a magnetic dot.

For negative applied fields, which generate anti-vortices with respect to the direction of the magnetization of the triangle, the symmetry of the triangle does not have a major influence on the nucleation process. Namely, for such field polarity, the triangle and external field induce opposite supercurrents in the disk, which tend to cancel each other. With increasing negative applied field, the vortex-like currents prevail and after the critical conditions are reached antivortices nucleate. The onset occurs through the GVS, as imposed by the cylindrical symmetry of the disk. For positive applied fields, on the other hand, there exists a competition between the cylindrical symmetry of the superconducting disk and the C_3 symmetry of the magnetic triangle, which governs the onset. Both currents, induced by the externally applied field and by the triangle, compress the vortices to the centre of the disk, but

imposing different geometries on the final vortex configuration. For $L = 1$ and $L = 2$, the distribution of the order parameter is influenced by the symmetry of the magnetic triangle through the suppression of the order parameter under its edge [11], but there is no particular correspondence between the vortex patterns and the symmetry of the stray field. For $L = 3$, however, the C_3 symmetry of the triangle has a pronounced influence and the GVS splits into three Φ_0 -vortices. This splitting is caused by the tendency of the system to minimize its kinetic energy, associated with the screening currents. This process can be thought of as the competition between the triangularly imposed confinement, compressing vortices to its centre and their mutual repulsion. Therefore, due to the C_3 symmetry, only the state $L = 3$ may actually be stabilized as a collection of Φ_0 -vortices. The vortices assume the positions close to the apices of the triangle, where the positive stray field is the highest.

Given that the specific distribution of the screening currents following from the shape of the triangle, the configuration of the three Φ_0 vortices which minimizes the kinetic energy remains favourable and stable in a broad range of applied fields, that is, the three vortices are strongly pinned at their positions. The enhanced temperature stability range follows from the size constraints of the pinning site. Namely, the fourth vortex can only enter under the triangle when the pinning area becomes large enough in terms of $\xi(T)$, so that the pinning force overwhelms the vortex-repulsion. The fourth vortex is then pushed to the centre of the triangle, without causing any substantial rearrangement of the three vortices. For vorticity $L = 5$ three Φ_0 -vortices remain stable and pinned at the apices of the triangle, whereas a GVS with vorticity 2 is created at the centre of the triangle. For higher fields, the vortices below the triangle merge, forming a single GVS state. This is the first time that such a reentrant behaviour at the phase boundary has been observed.

In conclusion, we have investigated the onset of superconductivity in a mesoscopic superconducting disk with a perpendicularly magnetized magnetic triangle. We demonstrated that the symmetry of the magnetic triangle strongly affects the nucleation process. For applied field oriented antiparallel to the magnetization of the triangle, the nucleation of superconductivity is predominantly influenced by the boundary of the disk and occurs through the GVS, whereas for fields applied parallel to the magnetic moment of the triangle the GVS with vorticity $L = 3$ splits into three Φ_0 -vortices. This magnetically induced explosion of the GVS is generally applicable to mesoscopic superconductors with magnetic polygons on top, where the number of apices would determine the particular vorticity at which the GVS splits into a set of Φ_0 vortices.

This work was supported by the Research Fund K. U. Leuven GOA/2004/02 programme, the University of Antwerp (GOA), the Flemish FWO and the Belgian IUAP programmes, as well as by the JSPS/ESF "Nanoscience and Engineering in Superconductivity" programme.

-
- [1] V. V. Moshchalkov *et al.*, Nature **373**, 319 (1995).
 - [2] V. A. Schweigert, F. M. Peeters and P. S. Deo, Phys. Rev. Lett. **81**, 2783 (1998); A. K. Geim *et al.*, Nature (London) **390**, 259 (1997); V. Bruyndoncx *et al.*, Phys. Rev. B **60**, 10468 (1999); A. Kanda *et al.*, Phys. Rev. Lett. **93**, 257002 (2004).
 - [3] L. F. Chibotaru *et al.*, Nature (London) **408**, 833 (2000); *ibid.* Phys. Rev. Lett. **86**, 1323 (2001); V. R. Misko *et al.*, Phys. Rev. Lett. **90**, 147003 (2003).
 - [4] F. M. Peeters and V. A. Schweigert, Phys. Rev. B **63**, 144517 (2001); W. V. Pogosov, *ibid.* **65**, 224511 (2002).
 - [5] M. V. Milošević, S. V. Yampolskii and F. M. Peeters, Phys. Rev. B **66**, 024515 (2002)
 - [6] D. S. Golubović *et al.*, Phys. Rev. B **68**, 172503 (2003)
 - [7] D. S. Golubović *et al.*, Europhys. Lett. **65**, 546 (2004).
 - [8] A. Y. Aladyshkin, A. S. Mel'nikov and D. A. Ryzhov, J. Phys.: Condens. Matter **38**, 6591 (2003); J. E. Villegas *et al.*, Science **302**, 1188 (2003); M. Lange *et al.*, Phys. Rev. Lett. **90**, 197006 (2003).
 - [9] P. F. Carcia, J. Appl. Phys. **63**, 10 (1998); J. V. Harzer *et al.*, *ibid.* **69**, 2448 (1991).
 - [10] V.A. Schweigert and F.M. Peeters, Phys. Rev. B **57**, 13817 (1998).
 - [11] M. V. Milošević and F. M. Peeters, Phys. Rev. B **68**, 094510 (2003); *ibid.* Phys. Rev. B **69**, 104522 (2004).